Korean J. Chem. Eng., 34(4), 987-996 (2017)
DOI: 10.1007/s11814-017-0006-4

pISSN: 0256-1115
eISSN: 1975-7220

Process optimization and kinetic modeling for esterification of propionic acid with benzyl alcohol on ion-exchange resin catalyst

Vishal Suresh Chandane, Ajit Pralhad Rathod†, Kailas Lachchhuram Wasewar, and Shriram Shaligram Sonawane

Department of Chemical Engineering, Visvesvaraya National Institute of Technology, Nagpur- 440010 (MS), India

(*Received 10 May 2016 • accepted 5 January 2017*)

Abstract–Benzyl propionate, an ester with floral and fruity odor, has significant applications in perfumery and flavor industries. This paper describes the optimization of the synthesis of benzyl propionate catalyzed by Amberlyst-15. The effects of various process parameters such as catalyst loading, alcohol-to-acid molar ratio and reaction temperature on propionic acid conversion and yield of ester were assessed by response surface methodology (RSM). The external and internal mass transfer limitations were found to be absent. Analysis of variance (ANOVA) showed that the acquired quadratic model successfully interpreted the experimental data with the coefficient of determination values, (R^2>0.98) and adjusted R^2 values, (>0.97). The RSM model was validated by good agreement between the model predicted and experimental values for responses. Pseudohomogeneous (PH) kinetic model was used and validated (R^2>0.95) with the experimental data. The activation energy and frequency factor were evaluated as 42.07 kJ mol^{-1} and 19,874.64 L mol^{-1} min^{-1}, respectively.

Keywords: Benzyl Propionate, Optimization, Response Surface Methodology, Box-Behnken Design, Kinetics

INTRODUCTION

Organic esters find significant applications in a wide range of chemical applications, including flavors, fragrances, solvent additives, plasticizers, medicinal and surface-active agents [1]. Thousands of different types of esters are commercially produced for variety of applications. A number of routes are available for the synthesis of organic esters [2] but; the simplest and common way to produce esters is the direct esterification of carboxylic acids and alcohols in presence of homogeneous or heterogeneous catalyst.

In general, esterification reactions are accompanied by slow reaction rates and are limited by chemical equilibrium [3]. A catalyst is used to enhance the reaction rate. The homogeneous catalyst includes strong mineral acids such as H_2SO_4, HCl, *p*-toluene sulfonic acid and methanesulfonic acid. Although, they have strong catalytic activity but also have drawbacks of equipment corrosion, side reactions and require one more step of product purification. Due to these limitations, heterogeneous catalysts have gained more attention in the past years. They have several benefits, such as easy separation from reaction mixture, high product purity and elimination of both corrosive environment as well as the side reactions. Thus, heterogeneous catalysts are preferred for esterification reactions. They include many solid acids and bases, zeolites, ion exchange resins, supported catalyst and clay catalyst [4-10].

Ion exchange resins are the most commonly used heterogeneous catalysts for the esterification reaction. They are selective in adsorption of reactants and possess swelling nature. Owing to this, they not only catalyze but also affect the equilibrium conversion of esterification reaction [11]. For the studies demonstrating to ion exchange resins, readers may refer to several earlier works [12-21]. Amberlyst-15 has a strong catalytic activity and is commonly applied as a catalyst for various esterification reactions reported in the literature.

Response surface methodology (RSM) is an efficient mathematical and statistical method for experimental design, developing models, optimizing multifactor experiments and evaluating optimal operating condition for a reaction system. It is a time saving tool that helps the user to collect a large amount of information by performing a small number of experiments. In addition, it provides the possibility of observing the effect of individual variables and their combinations of interactions on response variable [22].

Benzyl propionate, discussed in this study, is a colorless clear oily liquid with an odor reminiscent of banana, apricot and pineapple. Due to these properties, it is widely used in chemical industries for flavoring certain food products and as a modifier in many perfumeries. At present, no information is available in literature depicting the esterification of propionic acid with benzyl alcohol in presence of ion exchange resin catalysts. The detailed reaction mechanism for the esterification of propionic acid with benzyl alcohol to produce benzyl propionate and water is given as Scheme 1 and explained as follows [23]:

- Protonation of carbonyl oxygen of propionic acid (P.A.) by acid catalyst to form carbocation;
- Nucleophilic attack at positive carbon of carbocation by the hydroxyl group of benzyl alcohol (B.A.);
- Transfer of proton from hydroxyl group of benzyl alcohol (B.A.) to carbonyl oxygen of propionic acid (P.A.);
- Delocalization of positive charge, loss of water and formation of reaction intermediate;
- Stabilization of reaction intermediate, production of benzyl propionate (B.P.) and regeneration of acid catalyst.

---

†To whom correspondence should be addressed.
E-mail: ajitprathod@gmail.com

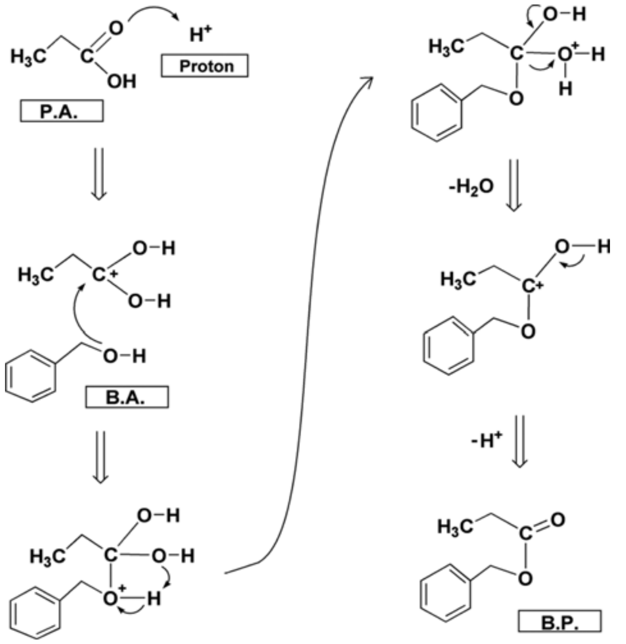

Scheme 1. **Reaction mechanism for esterification of propionic acid with benzyl alcohol.**

The present study deals with the esterification of propionic acid with benzyl alcohol in presence of Amberlyst-15 as catalyst. Multi-response-based RSM analysis was employed in the study and the interaction of various process parameters on the two response variables were investigated and optimized. The three critical process variables namely catalyst loading, molar ratio of alcohol to acid and reaction temperature, and two response variables--conversion of propionic acid and yield of ester, were studied using Box-Behnken experimental design (BBD), and subsequently an empirical mathematical model correlating process and response variables was developed. The kinetics of the esterification reaction was studied at the optimized process parameters obtained from RSM model. In present study, the liquid concentration was used instead of the activity of each component for the development of kinetic model. It is built on the assumptions that the rate of the non-catalyzed reactions is negligible compared with the catalyzed reactions, the catalytic activity of all sites on the surface of the catalyst surface is the same, and the complete reaction system is assumed as an ideal solution [24-26]. Amberlyst-15 was the source of proton and the model was developed by employing the reaction mechanism presented in Scheme 1. The adsorption of reactant and product on catalyst surface was assumed to be weak and the surface reaction was assumed to be the rate determining step. Under these conditions, a pseudohomogeneous (PH) second-order model was assumed and chosen to simulate the experimental data.

EXPERIMENTAL

1. Chemicals

Propionic acid (purity >99%) and benzyl alcohol (purity >99%) were obtained from Merck and used without further purification. Methanol and Karl Fischer reagent were procured from Rankem Chem. Ltd. India. Ion exchange resin Amberlyst 15 (dry), a product of Rohm and Haas was purchased from S.D. fine chem. Ltd. Mumbai. Resin was dried to remove moisture content if any. The physicochemical properties of catalyst are listed in Table 1.

Table 1. Physico-chemical properties of Amberlyst 15

Matrix type	Styrene-divinylbenzene
Physical form	Grey spherical beads
Ionic form	H^+ form
Ion exchange capacity (meq/g of dry catalyst)	4.7
Surface area (m^2/g)	53
Particle size (mm)	0.600-0.800
Pore Volume (cm^3/g)	0.40
Maximum operating temperature	120
Operating pH range	0-14
Moisture holding capacity	52-57%

2. Experimental Procedure

The ion exchange capacity of Amberlyst 15 resin was measured experimentally. In a typical test, 1 g of dried resin was taken in a conical flask containing 50 cm^3 of 1 N sodium chloride solution. The flask was ultrasonicated for 1 h. After that, the resin was filtered and the filtrate solution was titrated against 0.1 N sodium hydroxide solution using phenolphthalein as an indicator. The ion exchange capacity was estimated as an average of three measurements and found to be 4.3±0.05 meq/g, which was in accordance with the value stated by the manufacturer.

The batch experiments were carried out in a 250 cm^3 three neck flask provided with reflux condenser and magnetic stirrer. The flask was heated on a rotamantle (Remi 1RML) and the temperature was maintained within accuracy of ±0.2 °C with the help PID temperature controller. The alcohol and catalyst were first charged into the flask and heated to the desired temperature followed by the charging of propionic acid at the same temperature which was heated separately. The time at which heated propionic acid charged was taken as zero time. Aliquots of samples were collected for every 15 min for first two hours and for every 30 min for further hours.

3. Analysis

All experiments were performed in triplicate to ensure the reproducibility of results. The amount of propionic acid in the reaction mixture was determined by titrating with 0.1 N sodium hydroxide solution using phenolphthalein as an indicator. The water content in the reaction mixture was evaluated by micro-processor based Karl Fischer titrator (Optics Technology, India). After ensuring that the measured water content corresponded to the calculated values of stoichiometric equation, it was confirmed that there were no side reactions.

4. Experimental Design and Mathematical Model

Response surface methodology (RSM) was used to investigate the operating parameters of esterification to obtain high % conversion of propionic acid and high yield of ester. An experimental design was developed by selecting three independent process variables at three levels, and the factors considered included catalyst loading (X_1), molar ratio of alcohol to acid (X_2) and reaction temperature (X_3). The % conversion of propionic acid (Y_1) and yield of ester

Table 2. Coded levels for independent variables used in Box-Behnken design

Variables	Symbol	Coded levels		
		−1	0	+1
Catalyst loading (% wt/wt)	X_1	1	4	7
Molar ratio of alcohol to acid (M)	X_2	2	5	8
Reaction temperature (K)	X_3	353	363	373

(Y_2) were selected as response variables for the experimental design. Seventeen sets of experiments (12 factorial and 5 center points) were performed according to standard Box-Behnken experimental design. For each independent variable, the experimental range and central point are listed in Table 2. The Design Expert Version 9.0.6 (US, State-Ease Inc.) software was used for designing and evaluating the experimental data.

A second-order polynomial equation recommended by RSM was used to predict the optimum value and subsequently to reveal the interactions between the factors:

$$Y=\beta_0+\sum_{i=1}^{k}\beta_i X_i+\sum_{i=1}^{k}\beta_{ii} X_i^2+\sum_{i=1}^{k}\beta_{ij} X_i X_{ij}+e \qquad (1)$$

where, Y denotes the response variable, X_i denotes the coded levels of independent variables. β_0, β_i, β_{ii}, β_{ij} represents the regression coefficients, the linear terms, squared terms for the variables i, and interaction terms between i and j, respectively. X_i, X_{ii} and X_{ij} denote the linear, quadratic and interactive terms of the coded independent variables, respectively. The k is the total number of variables used to optimize the propionic acid conversion and e is the random error.

RESULTS AND DISCUSSION

1. Mass Transfer Considerations

The influence of external mass transfer resistance on the esterification reaction was evaluated by performing the experiments under similar operating conditions of 353 K temperature, M=2 and catalyst loading of 1% (wt/wt) at different stirrer speeds of 200, 500 and 800 rpm. Results are given in Fig. 1, which indicated that reaction rate as followed by conversion of propionic acid did not significantly differ by varying the stirrer speed. Particularly, for stirrer speeds above 500 rpm, the differences were considered to be negligible. This indicated the absence of external mass transfer resistance above 500 rpm and hence, all experiments were carried out at a stirrer speed of 500 rpm to avoid the influence of external mass transfer limitations.

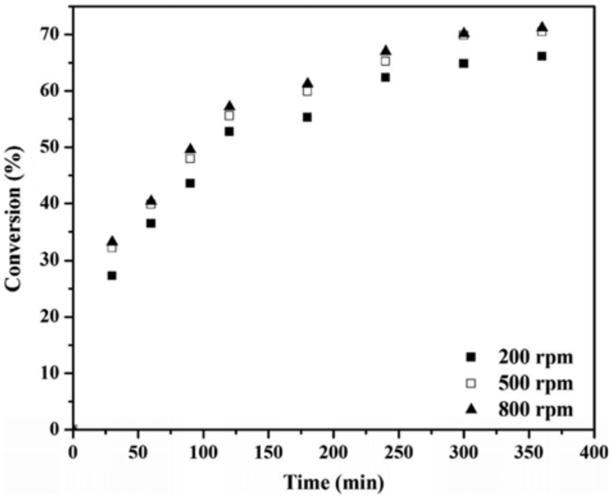

Fig. 1. Conversion of esterification reaction at different stirrer speeds.

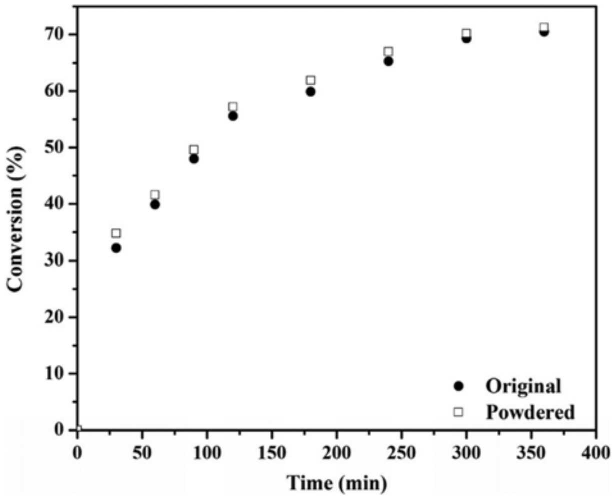

Fig. 2. Conversion of esterification reaction for catalyst in original form and for catalyst in powdered form.

To investigate the influence of internal mass transfer resistance on the esterification reaction, experiments were conducted under similar operating conditions as mentioned earlier by using the catalyst in original form and by converting the catalyst into powdered form. Results are given in Fig. 2, which shows that the reaction rate as followed by conversion was almost independent of particle size of catalyst. This indicated that the reaction was not internal diffusion controlled.

These results are in accordance with the literature reports stating that the esterification reactions catalyzed by Amberlyst series resins are not controlled by external and internal diffusion [18,19, 27-29].

2. RSM Analysis

2-1. Model Determination

The statistical summary for each model that was given by Design Expert software is presented in Table 3. The R^2 and Adj-R^2 values for linear relationship are 0.4435 and 0.3150 respectively, which showed that the linear relationship was not adequate for the experimental data. A quadratic model is suggested by the software, even though

Table 3. Statistical summary for each model

Model	Sum of squares	R^2	Adjusted R^2	Suggestion
Linear	121.71	0.4435	0.3150	Not adequate
Quadratic	89.22	0.9884	0.9734	Suggested
Cubic	3.20	1.00	1.00	Aliased

it has lower R^2 and Adj-R^2 values because the cubic model is aliased, which means that the effects of each variable which causes different signals become indistinguishable. Thus, the quadratic model was selected to fit the experimental data.

2-2. Model Fitting and Analysis of Variance (ANOVA)

Experiments were performed according to standard Box-Behnken experimental center-united design (BBD) in a randomized order to avoid bias. The results obtained after conducting 17 sets of experiments for the fixed reaction time of 6 hr in triplicate are presented in Table S1 (Supporting Information). Multiregression and backward elimination were used to determine the best fitting model. Table S1 also represents the values of propionic acid conversion and yield of ester that was predicted by the software.

The second-order quadratic relationship between process and response variables based on RSM analysis is expressed as;

$$Y_1=-83.60+11.21X_1+9.13X_2+2.81X_3-0.44X_1^2-0.14X_2^2 -0.013X_3^2-0.33X_1X_2-0.059X_1X_3-0.058X_2X_3 \quad (2)$$

$$Y_2=-77.54+11.20X_1+8.70X_2+2.68X_3-0.43X_1^2-0.12X_2^2 -0.012X_3^2-0.32X_1X_2-0.059X_1X_3-0.057X_2X_3 \quad (3)$$

where, Y_1 is the propionic acid conversion and Y_2 is yield of ester.

The coefficients with positive sign in linear terms indicates that the conversion of propionic acid and yield of ester increases linearly with increase in variable i.e., synergistic effect, whereas coefficients with negative sign show antagonistic effect [30-32]. From Eqs. (2) and (3), the linear coefficient of the catalyst loading (X_1) has the highest value among the linear coefficients of other variables. This reveals that the catalyst loading has the strongest effect on the conversion of propionic acid and yield of ester. The next term which exhibits significant effect on the conversion of propionic acid and yield of ester is the molar ratio of alcohol to acid (X_2), followed by the temperature (X_3) which has least value. The interaction effects between parameters (X_1X_2) were observed to be highly significant, whereas slightly weaker interaction effects between parameters (X_1X_3) and (X_2X_3) were observed. This may be due to the cumulative effects of reaction parameters; similar results are reported in the literature [22,24].

Tables S2 and S3 illustrate the ANOVA test results of the acquired model. The ANOVA test provides the statistical significance of each effect within the experimental range by comparing with the mean square and the estimated error. To evaluate the goodness of model, the coefficient of variation and the F-value test was also performed. The F-value reported in Tables S2 and S3 is the ratio of model mean square to the appropriate mean square error. The F-value test uses the p-value standard to determine the significance of regression coefficients. The model F-values of 66.02 and 71.02 implied that the model was significant and there was only 0.01% chance that an F-value this large could occur due to noise. The p-value <0.05 indicates the significant model terms. In this case all linear, quadratic and interaction effects were significant model terms.

The coefficient of determination values (R^2) of 0.9884 and 0.9892 revealed that the models could explain 98.84% and 98.92% of the variability, respectively. The predicted R^2 values of 0.8137 and 0.8271 are in reasonable agreement with the adjusted R^2 values of 0.9734 and 0.9752, respectively, as their difference is less than 0.2. An adequate precision value indicates the signal-to-noise ratio. Generally, a ratio greater than 4 is desirable for the model to be used efficiently. In the present case, ratios of 32.361 and 33.735 indicate an adequate signal; hence, this model can be used to navigate the design spaces.

2-3. Model Accuracy Check

Since an accuracy check is essential to get an adequate model, we checked by comparing the experimental and model predicted values of propionic acid conversion and yield of ester. Fig. 3(a) and (b) depicts a good linear correlation between predicted and experimental values of propionic acid conversion and yield of ester. Additionally, a normal plot of residuals was obtained between the normal probability (%) and the internally studentized residuals. The internally studentized residuals measure the standard deviations separating the experimental and predicted values [33]. A good linear agreement between the normal probability (%) and the internally studentized residuals [Supporting Information, (Fig. S1 and Fig. S2)] shows that no response transformation was required and there was no apparent problem with normality.

2-4. Response Analysis

The relationships between the two response variables and three selected parameters are presented in Figs. 4-9. Each plot indicates

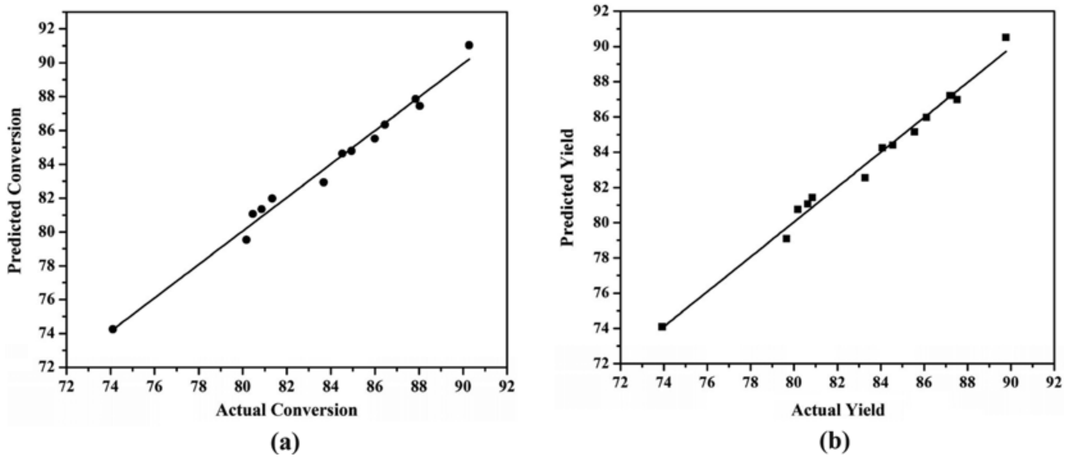

(a)

(b)

Fig. 3. Predicted vs. experimental values of (a) propionic acid conversion; (b) yield of ester.

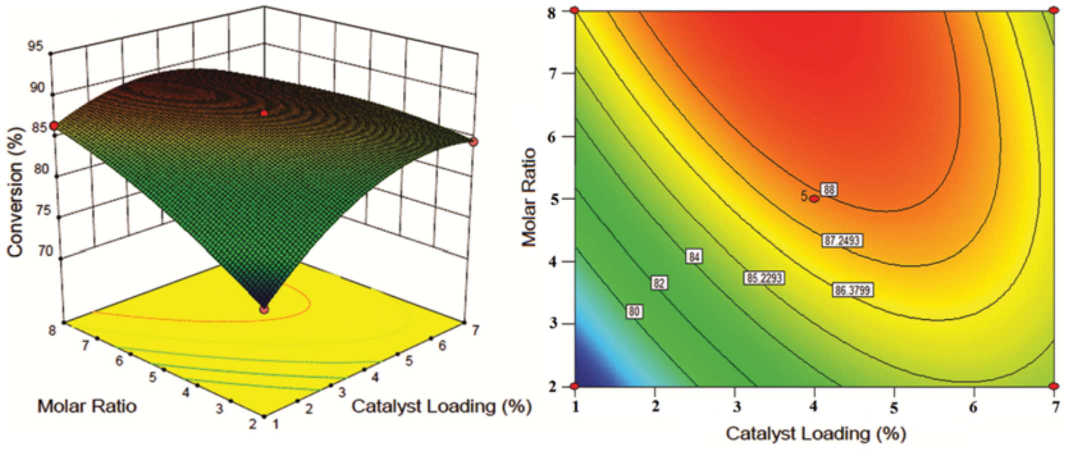

(a) (b)

Fig. 4. Effect of molar ratio and catalyst loading on conversion of propionic acid with temperature at the zero level: (a) Response surface plot; (b) contour plot.

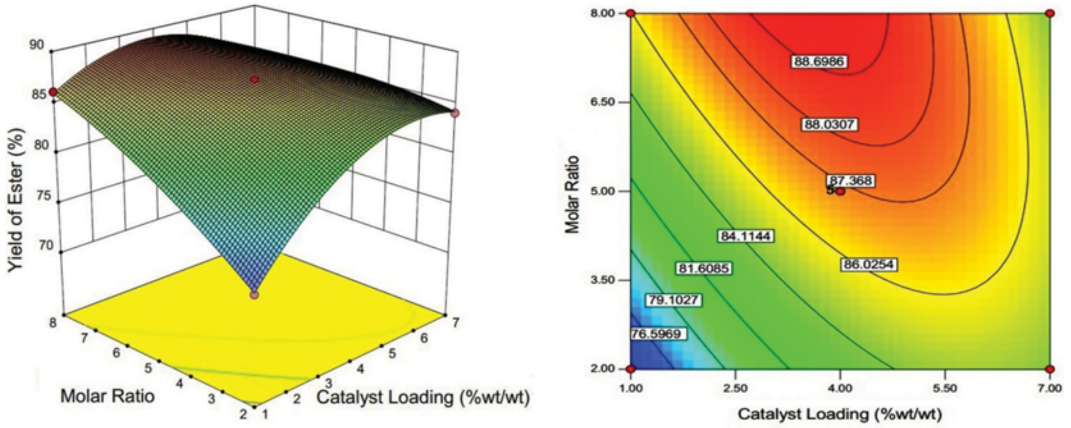

(a) (b)

Fig. 5. Effect of molar ratio and catalyst loading on yield of ester with temperature at the zero level: (a) Response surface plot; (b) contour plot.

the interaction of two parameters within their ranges on the response variable by keeping the other variable at its zero level. The response surfaces of the model better visualize the tendency of each factor to influence the conversion. Eqs. (2) and (3) were used to generate the three-dimensional (3D) response surface plots and two-dimensional (2D) contour plots. The shape of contour plots depicts the nature and extent of the interactions between the parameters. The interaction between corresponding parameters becomes prominent when the contour plot is elliptical, while it becomes negligible when the contour plot is circular.

Fig. 4(a) and (b) illustrates the effects of interaction between catalyst loading and molar ratio of alcohol to acid on propionic acid conversion. As can be seen from Fig. 4(a) and (b), enhancing the amounts of catalyst could bring about higher conversion of propionic acid. Similarly, the conversion of propionic acid increased with increasing the molar ratio. It implies that both, catalyst loading and molar ratio, had a significant effect on the conversion of propionic acid. This result also is supported with lower p-value (<0.0001) of interaction term X_1X_2 (Table S2) and positive coefficients of linear terms of X_1 and X_2 (Eq. (2)). Similarly, the interaction of these parameters on yield of ester is shown in Fig. 5(a) and (b). It was observed that the interaction between catalyst loading and molar ratio had strong effect on yield of ester. The high catalyst loading with more amounts of reactants increases the mass transfer rate, which subsequently increases the product yield. The elliptical shape of contour plot and a very low p value (<0.0001) of interaction term X_1X_2 (Table S3, Supporting Information) reveals the significance of this interaction effect.

Fig. 6(a) and (b) shows the effects of interaction between catalyst loading and temperature on propionic acid conversion. Reaction temperature plays a significant role in determining the reaction rates of esterification reaction [25]. It is evident from the Fig. 6(a) and (b) that at lower temperature, the enhancing amounts of catalyst brings higher conversion of propionic acid. However, at higher temperature, the conversion of propionic acid does not show significant increase. This might be due to the slight deactivation of

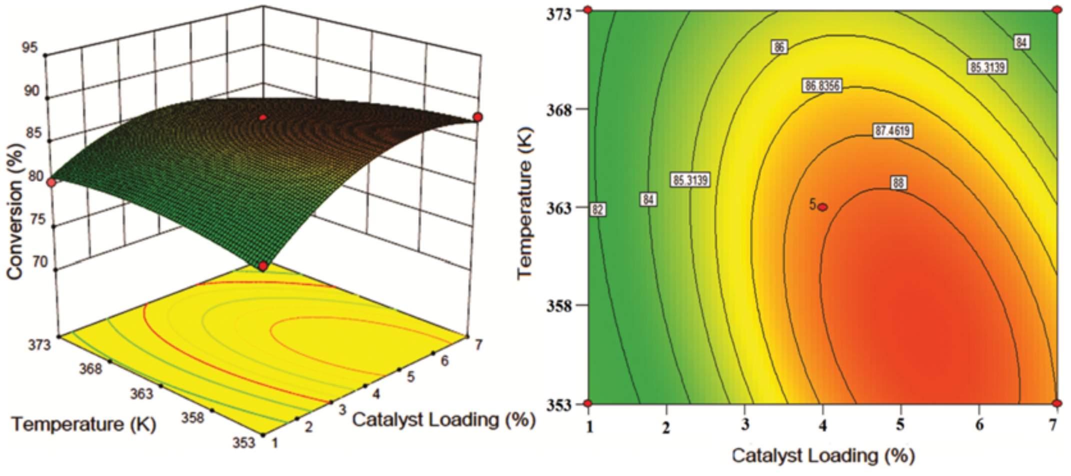

(a) (b)

Fig. 6. Effect of temperature and catalyst loading on conversion of propionic acid with molar ratio at the zero level: (a) Response surface plot; (b) contour plot.

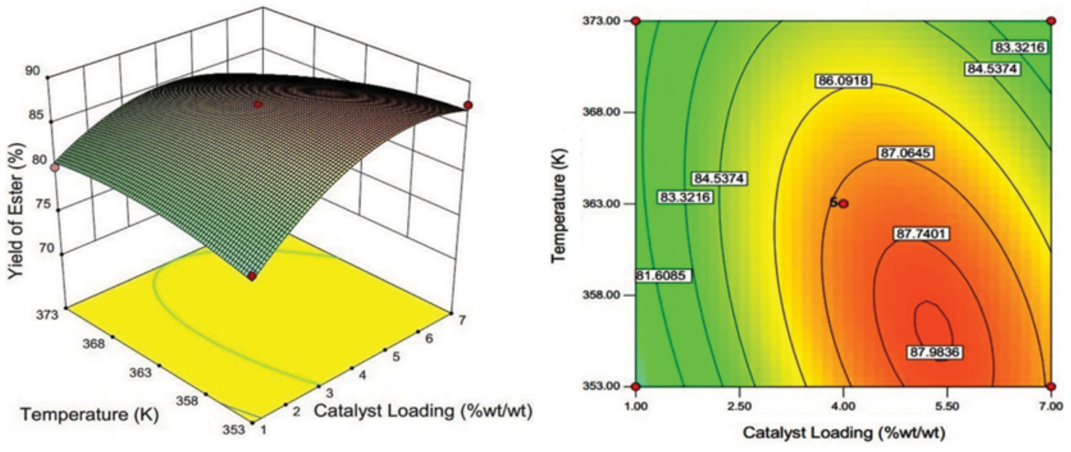

(a) (b)

Fig. 7. Effect of temperature and catalyst loading on yield of ester with molar ratio at the zero level: (a) Response surface plot; (b) contour plot.

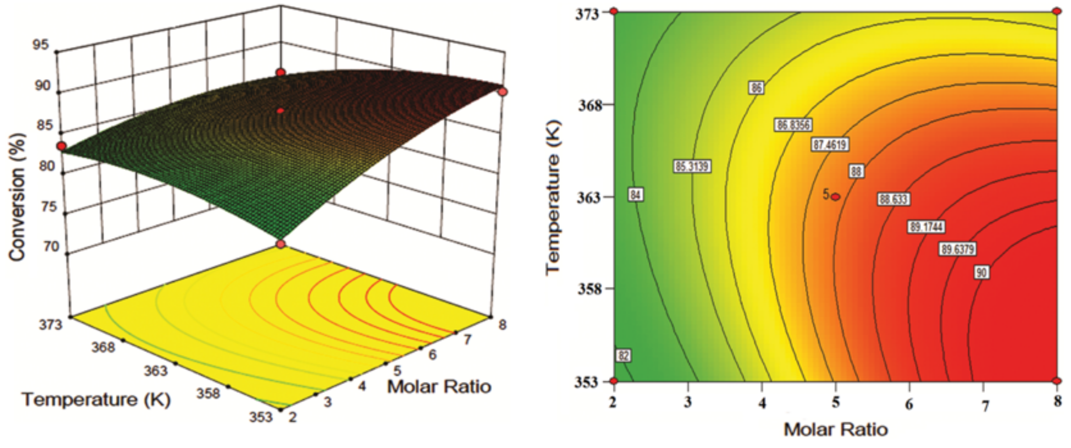

(a) (b)

Fig. 8. Effect of temperature and molar ratio on conversion of propionic acid with catalyst loading at the zero level: (a) Response surface plot; (b) contour plot.

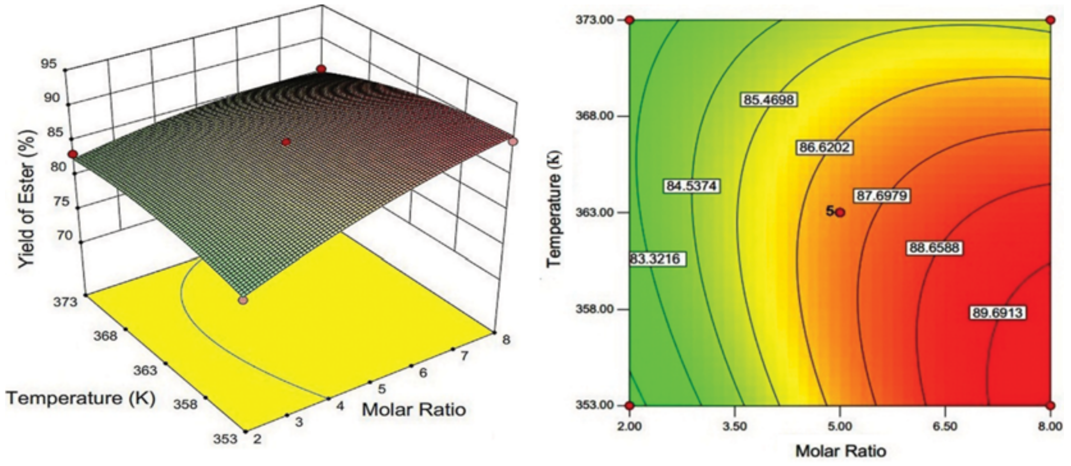

(a) (b)

Fig. 9. Effect of temperature and molar ratio on yield of ester with catalyst loading at the zero level: (a) Response surface plot; (b) contour plot.

catalyst at higher temperature. In addition, Fig. 7(a) and (b) shows the interaction between catalyst loading and temperature on yield of ester. Enhancing the catalyst amount and temperature enhances the yield of ester; however, a marginal enhancement in yield is observed at higher temperature. A circular contour plot and a lower p value (0.0008) of interaction term X_1X_3 (Table S3, Supporting Information) illustrates that the interaction effect of catalyst loading and temperature on yield of ester is considerably significant.

Fig. 8(a) and (b) illustrates the effects of interaction between molar ratio of alcohol to acid and temperature on propionic acid conversion. In Fig. 8(a) and (b), the propionic acid conversion increased proportionally with molar ratio at any temperature from 353 to 373 K. This means that reaction temperature exhibited less effect on the conversion at different molar ratios. This result also is supported with lower value of coefficient of linear term of X_3 (Eq. (2)). The contour plot shows the prominent interaction between these two variables. Likewise, the interaction between molar ratio of alcohol to acid and temperature on yield of ester is presented in Fig. 9(a) and (b). The increase in molar ratio increases the product yield proportionally with the increase in temperature. However, at higher temperature very slight increase in yield of ester was noted. The interaction effects of these two parameters were observed to be significant with the elliptical nature of contour plot and lower p value (0.0010) of interaction term X_2X_3 (Table S3, Supporting Information).

2-5. Optimization of Process Parameters

The optimum values for selected parameters were evaluated from the numerical feature of Design Expert Version 9.0.6 software. In numerical optimization, the selected parameters, namely catalyst loading, alcohol to acid molar ratio and temperature, were set within the coded range between low (−1) to high (+1) (Table 3), while the propionic acid conversion and yield of ester was set to maximize the value between minimum and maximum (See Table S1). Subsequently, 100 solutions for optimum conditions were found by software and the solution with highest desirability was selected to confirm the prediction of the model. The optimum conditions, including predicted and experimental values for propionic acid conversion and yield of ester, are listed in Table 4. The experimental value reported in Table 4 is the average of three independent experimental values, which is in reasonable agreement with the predicted values. Thus, response surface methodology with Box-Behnken design with a quadratic model was found to be adequate and statistically accurate to optimize the esterification of propionic acid and benzyl alcohol.

Table 4. Optimum process conditions for the esterification reaction and model validation

Parameters	X_1	X_2	X_3	Y_1	Y_2
Predicted	4.27	7.82	353.37	90.95	89.17
Experimental	4.5	8	353	91.32±0.46	87.18±1.44

3. Kinetic Model

The esterification reaction of propionic acid (PA) with benzyl alcohol (BA) for producing benzyl propionate (BP) and water (W)

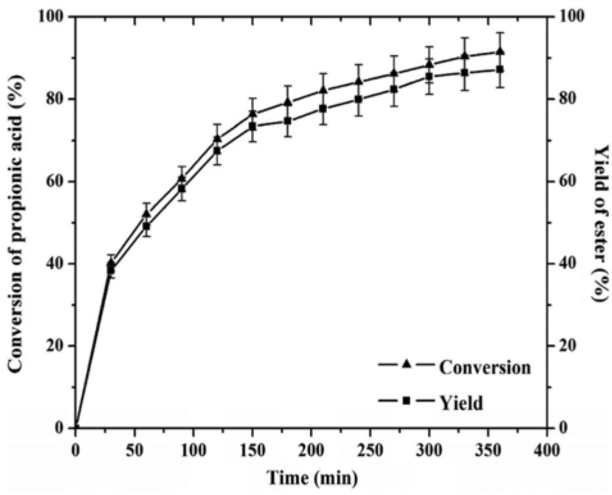

Fig. 10. Conversion and yield of esterification reaction under optimal process conditions.

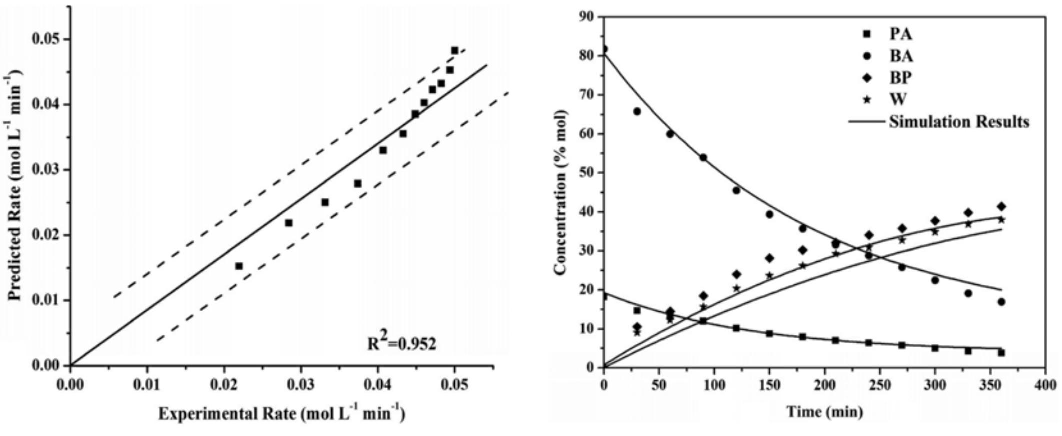

(a) (b)

Fig. 11. Pseudohomogeneous (PH) model plot of esterification reaction under of propionic acid and benzyl alcohol under optimal process conditions: (a) Parity plot between experimental and model predicted rate, (b) change of components concentration of reaction mixture vs. time, experimental vs. model predicted results.

in the presence of Amberlyst-15 catalyst is given as follows:

$$\mathrm{PA+BA \rightleftharpoons BP+W} \tag{4}$$

An independent experiment was conducted under optimized operating conditions (Table 4) for the kinetic study, and the results are represented in Fig. 10. In absence of the internal and external mass transfer limitations and large excess of benzyl alcohol as compared with propionic acid was present, the formation of benzyl propionate (BP) can be divided into three individual steps [23]:

$$\mathrm{PA+S \rightleftharpoons PA{\cdot}S;} \qquad -r_1=k_1C_{PA}C_S-k_{-1}C_{PAS} \tag{5}$$

$$\mathrm{PA{\cdot}S+BA \rightleftharpoons BP{\cdot}S+W;} \qquad -r_2=k_2C_{PAS}C_{BA}-k_{-2}C_{BPS}C_W \tag{6}$$

$$\mathrm{BP{\cdot}S \rightleftharpoons BP+W;} \qquad -r_3=k_2C_{BPS}C_{BA}-k_{-3}C_{BP}C_S \tag{7}$$

where C_{PA}, C_{BA}, C_{BP} and C_W refer to the concentration of propionic acid, benzyl alcohol, benzyl propionate and water, respectively. k_1 k_2 k_3 and k_{-1} k_{-2} k_{-3} are the kinetic constants for forward and reverse reaction, respectively.

It was considered that the surface reaction is the rate determining step, and then the overall rate can be expressed as

$$-r_a=-r_2=k_2K_1C_t(C_{PAS}C_{BA}-k_{-2}C_{BPS}C_W/K_{eq})/(1+K_1C_{PA}+K_{-3}C_{BP}) \tag{8}$$

where, K_{eq} is equilibrium constant for the esterification reaction. The experiment was performed at optimized operating condition for 24 hrs and the equilibrium constant was calculated by using Eq. (9):

$$K_{eq}=(C_{BP}C_W/C_{PA}C_{BA})=X_{eq}^2/(1-X_{eq})(M-X_{eq}) \tag{9}$$

We also assumed that the adsorption of propionic acid on catalyst surface was weak and thus K_1 and K_{-3} could be assumed to be negligible. Thus, Eq. (8) could be transformed as:

$$-r_a=-r_2=k_a(C_{PAS}C_{BA}-k_{-2}C_{BPS}C_W/K_{eq}),\ k_a=k_2K_1C_t \tag{10}$$

The reaction rate constant, k_a can be calculated by using Eq. (10) by means of regression method for the data obtained at optimized process conditions. The reaction rate was also calculated by using the derived model equation using Eq. (10). A parity plot of rates calculated by experiment and derived model is presented in Fig. 11(a). All the experimental data was in good agreement with the model predicted data. The solid line represents the goodness of fit (R^2=0.952), and the dashed line represents the 95% confidence interval. Additionally, using the kinetic model equation, the change of components concentration was calculated under optimized process conditions and plotted against time. It is evident from Fig. 11(b) that the experimental and model predicted results are in good agreement. This reveals that the PH kinetic model is valid for the esterification reaction [23,30,33-34].

The Arrhenius equation is used to express the temperature dependency of reaction and is expressed as Eq. (11). The rate constants were obtained at different reaction temperatures under optimized operating conditions (including optimized reaction temperature) using the kinetic model equation (Eq. (10)). A plot of $\ln k_a$ vs.

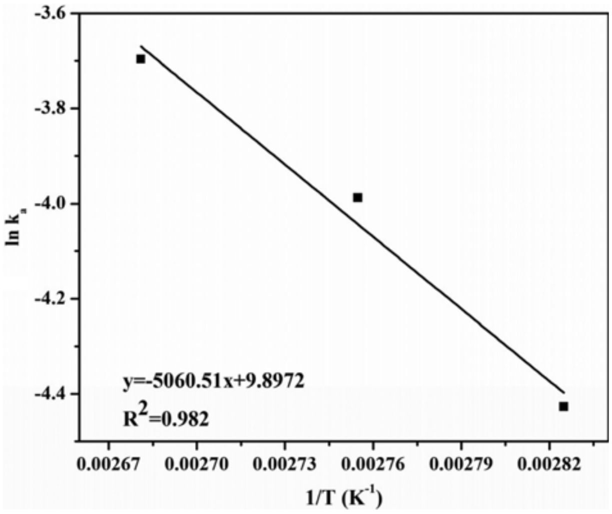

Fig. 12. Arrhenius plot of esterification of propionic acid and benzyl alcohol.

1/T presented in Fig. 12 indicates a straight line. The activation energy (E_i) and frequency factor (k_i^o) were evaluated by linear regression using the software Origin Pro 8.

$$\ln k = \ln k_i^o - \frac{E_i}{RT} \tag{11}$$

The activation energy and frequency factor for the esterification of propionic acid and benzyl alcohol were evaluated to be 42.07 kJ mol^{-1} and 19,874.64 L mol^{-1} min^{-1}, respectively. It was reported that diffusion-limited reactions show low activation energy (10-15 kJ mol^{-1}), whereas kinetically controlled reactions show activation energy excess [35,36]. Thus, in the present study, the high activation energy (42.07 kJ mol^{-1}) indicates that the esterification of propionic acid and benzyl alcohol is kinetically controlled.

CONCLUSIONS

The optimization of esterification of propionic acid with benzyl alcohol catalyzed by Amberlyst-15 was carried out in a batch reactor. The external mass transfer resistance was found to be absent at the stirrer speed of ≥500 rpm. The internal mass transfer limitation was assessed experimentally and found to be absent. The RSM with Box-Behnken center united design was used to optimize the various process parameters of esterification reaction with few numbers of experiments. A quadratic model was found to be significant for the esterification reaction, and it fitted the experimental data well, with a coefficient of determination values of, (R^2=0.9884 and R^2=0.9892) and an Adj-R^2 values of (0.9734 and 0.9752). Additionally, the p-value of this model was <0.0001, which revealed that the model is highly significant. At optimal process conditions of (catalyst loading of 4.27 (% wt/wt), molar ratio (alcohol to acid) of 7.82 and reaction temperature of 353.37 K), the predicted responses for conversion and yield were 90.95% and 89.17%. Experiments were carried out to verify the validity and accuracy of the model, and the results showed that the predicted value was in good agreement with the experimental values (91.32±0.46% and 87.18±1.44). Moreover, the kinetics was studied and second-order pseudohomogeneous (PH) model was used to simulate the experimental data. The developed kinetic model well predicted the experimental results. The esterification reaction was found to be kinetically controlled owing to high activation energy of 42.07 kJ mol^{-1} and the frequency factor was calculated as 19,874.64 L mol^{-1} min^{-1}.

NOMENCLATURE

X_1 : catalyst loading [% wt/wt]
X_2 : molar ratio of alcohol to acid
X_3 : reaction temperature [K]
Y_1 : conversion of propionic acid [%]
Y_2 : yield of ester [%]
β : regression coefficient
k : total number of variables
e : random error
S : active site surface
C_{PA} : concentration of propionic acid [mol/L]
C_{BA} : concentration of benzyl alcohol [mol/L]
C_{BP} : concentration of benzyl propionate [mol/L]
C_W : concentration of water [mol/L]
C_t : total concentration of surface sites [mol/L]
$-r_i$: Rate constant for component *i* [L mol^{-1} min^{-1}]
K_{eq} : equilibrium constants for reaction
k_1 k_2 k_3 : rate constants for forward reaction [L mol^{-1} min^{-1}]
k_{-1} k_{-2} k_{-3} : rate constants for reverse reaction [L mol^{-1} min^{-1}]
K_1 K_{-1} : surface reaction equilibrium constants [L mol^{-1} min^{-1}]
k_a : reaction rate constant [L mol^{-1} min^{-1}]
X_{eq} : equilibrium conversion of propionic acid [%]
M : alcohol/acid molar ratio
T : temperature [K]
R : gas constant [kJ mol^{-1} K^{-1}]
E_i : activation energy [kJ mol^{-1}]
k_i^o : frequency factor [L mol^{-1} min^{-1}]

SUPPORTING INFORMATION

Additional information as noted in the text. This information is available via the Internet at http://www.springer.com/chemistry/journal/11814.

REFERENCES

1. J. J. McKetta, *Encyclopedia of Chemical Processing and Design; Marcel Dekker*, New York (1983).
2. G. D. Yadav and P. H. Mehta, *Ind. Eng. Chem. Res.*, **33**, 2198 (1994).
3. H. Y. Lee, L. T. Yen, I. L. Chien and H. P. Huang, *Ind. Eng. Chem. Res.*, **48**, 7186 (2009).
4. A. E. R. S. Khder, *Appl. Catal. A: Gen.*, **343**(1-2), 109 (2008).
5. X. Qin, W. Zhao, B. Han, B. Liu, P. Lian and S. Wu, *Korean J. Chem. Eng.*, **32**, 1064 (2015).
6. L. Zhou, Y. Niu, J. Yang, C. Li, X. Guo, L. Li and T. Qiu, *Korean J. Chem. Eng.*, **33**(8), 2478 (2016).
7. H. Su, X. Wang, Y. G. Kim, S. B. Kim, Y. G. Seo, J. S. Kim and C. J. Kim, *Korean J. Chem. Eng.*, **31**(11), 2070 (2014).
8. S. B. Valdeilson, C. L. Ivoneide, F. A. C. Garcia, S. C. L. Dias and J. A. Dias, *Catal. Today*, **133-135**, 106 (2008).
9. C. S. M. Pereira, S. P. Pinho, V. M. T. M. Silva and A. E. Rodrigues, *Ind. Eng. Chem. Res.*, **47**, 1453 (2008).
10. V. T. M. M. Silva and A. E. Rodrigues, *Chem. Eng. Sci.*, **61**, 316 (2006).
11. P. E. Jagadeeshbabu, K. Sandesh and M. B. Saidutta, *Ind. Eng. Chem. Res.*, **50**, 7155 (2011).
12. M. Sharma, R. K. Wanchoo and A. P. Toor, *Ind. Eng. Chem. Res.*, **53**, 2167 (2014).
13. B. Schmid, M. Döker and J. Gmehling, *Ind. Eng. Chem. Res.*, **47**, 698 (2008).
14. H. T. R. Teo and B. Saha, *J. Catal.*, **228**, 174 (2004).
15. A. P. Toor, M. Sharma, G. Kumar and R. K. Wanchoo, *Bull. Chem. React. Eng. Catal.*, **6**, 23 (2011).
16. A. Izci and F. Bodur, *React. Funct. Polym.*, **67**, 1458 (2007).
17. S. H. Ali, A. Tarakmah, S. Q. Merchant and T. Al-Sahhaf, *Chem. Eng. Sci.*, **62**, 3197 (2007).
18. P. Delgado, M. T. Sanz and S. Beltrán, *Chem. Eng. J.*, **126**, 111 (2007).
19. V. J. Cruz, J. F. Izquierdo, F. Cunill, J. Tejero, M. Iborra, C. Fité and

R. Bringué, *React. Funct. Polym.*, **67**, 210 (2007).
20. A. K. Kolah, N. S. Asthana, T. Dung Vu, C. T. Lira and D. J. Miller, *Ind. Eng. Chem. Res.*, **47**, 5313 (2008).
21. J. A. Khan, Y. Jamal, A. Shahid and B. O. Boulanger, *Korean J. Chem. Eng.*, **33**(2), 582 (2016).
22. W. Chen, P. Yin, H. Chen and Z. Wang, *Ind. Eng. Chem. Res.*, **51**, 5402 (2012).
23. J. I. Yang, S. H. Cho, H. J. Kim, H. Joo, H. Jung and K. Y. Lee, *Can. J. Chem. Eng.*, **85**(1), 83 (2007).
24. W. Liu, P. Yin, X. Liu, W. Chen, H. Chen, C. Liu, R. Qu and Q. Xu, *Energy Convers. Manage.*, **76**, 1009 (2013).
25. K. Y. Nandiwale, P. S. Niphadkar, P. N. Joshi, S. K. Sonar, S. S. Deshpande, V. S. Patil and V. V. Bokade, *Appl. Catal. A: Gen.*, **460-461**, 90 (2013).
26. R. Tesser, M. D. Serio, M. Guida, M. Nastasi and E. Santacesaria, *Ind. Eng. Chem. Res.*, **44**, 7978 (2005).
27. M. Pera-Titus, M. Bausach, J. Tejero, M. Iborra, C. Fité, F. Cunill and J. F. Izquierdo, *Appl. Catal. A: Gen.*, **323**, 38 (2007).
28. W. Mao, X. Wang, H. Wang, H. Chang, X. Zhang and J. Han, *Chem. Eng. Process.*, **47**, 761 (2008).
29. V. S. Chandane, A. P. Rathod, K. L. Wasewar and S. S. Sonawane, *Korean J. Chem. Eng.*, **34**(1), 249 (2017).
30. K. Y. Nandiwale and V. V. Bokade, *Ind. Eng. Chem. Res.*, **53**, 18690 (2014).
31. P. Yin, L. Chen, Z. Wang, R. Qu, X. Liu, Q. Xu and S. Ren, *Fuel*, **102**, 499 (2012).
32. C. C. Liao and T. W. Chung, *Chem. Eng. Res. Des.*, **91**, 2457 (2013).
33. H. L. Liu and Y. R. Chiou, *Chem. Eng. J.*, **112**, 173 (2005).
34. C. H. Su, *Bioresour. Technol.*, **130**, 522 (2013).
35. A. Patel and V. Brahmkhatri, *Fuel Process. Technol.*, **113**, 141 (2013).
36. V. Brahmkhatri and A. Patel, *Appl. Catal. A: Gen.*, **403**, 161 (2011).

Supporting Information

Process optimization and kinetic modeling for esterification of propionic acid with benzyl alcohol on ion-exchanged resin catalyst

Vishal Suresh Chandane, Ajit Pralhad Rathod[†]**, Kailas Lachchhuram Wasewar, and Shriram Shaligram Sonawane**

Department of Chemical Engineering, Visvesvaraya National Institute of Technology, Nagpur- 440010 (MS), India

(*Received 10 May 2016 • accepted 5 January 2017*)

Table S1. Box-Behnken centre united design, experimental data and predicted values for three process variables at three levels

Run	Experimental variables			Propionic acid conversion (%)		% Yield of ester	
	X_1	X_2	X_3	Experimental	Predicted	Experimental	Predicted
1	4	5	363	87.85	87.85	87.19	87.21
2	4	8	373	86.00	85.51	85.57	85.15
3	4	5	363	87.85	87.85	87.29	87.21
4	1	8	363	86.45	86.34	86.12	85.97
5	4	2	353	80.86	81.35	80.64	81.06
6	4	5	363	87.85	87.85	87.19	87.21
7	4	2	373	83.68	82.93	83.28	82.55
8	1	2	363	74.11	74.26	73.93	74.09
9	7	5	353	88.04	87.44	87.53	86.96
10	4	8	353	90.28	91.03	89.78	90.51
11	4	5	363	87.85	87.85	87.19	87.21
12	1	5	373	80.46	81.06	80.18	80.75
13	4	5	363	87.85	87.85	87.19	87.21
14	1	5	353	80.17	79.53	79.66	79.08
15	7	5	373	81.34	81.98	80.85	81.43
16	7	2	363	84.52	84.63	84.08	84.23
17	7	8	363	84.94	84.79	84.56	84.40

Table S2. ANOVA for acquired model with propionic acid conversion as response variable

Source	Sum of squares	Degrees of freedom	Mean square	F-value	P-value	Characteristics
Model	271.27	9	30.14	66.02	<0.0001	Significant
X_1	38.94	1	38.94	85.30	<0.0001	
X_2	75.03	1	75.03	164.35	<0.0001	
X_3	7.74	1	7.74	16.96	0.0045	
X_1X_2	35.52	1	35.52	77.81	<0.0001	
X_1X_3	12.22	1	12.22	26.76	0.0013	
X_2X_3	12.60	1	12.60	27.61	0.0012	
X_1^2	68.17	1	68.17	149.33	<0.0001	
X_2^2	7.35	1	7.35	16.10	0.0051	
X_3^2	7.38	1	7.38	16.16	0.0051	
Residual	3.20	7	0.46			
Lack of fit	3.20	3	1.07			
Pure error	0	4	0.000			
Cor total	274.47	16				

R^2=0.9884; Adjusted R^2=0.9734

Predicted R^2=0.8137; Adequate precision=32.361

Table S3. ANOVA for acquired model with yield of ester as response variable

Source	Sum of squares	Degrees of freedom	Mean square	F-value	P-value	Characteristics
Model	257.395	9	28.60	71.02	<0.0001	Significant
	36.682	1	36.68	91.09	<0.0001	
	72.602	1	72.60	180.29	<0.0001	
	7.474	1	7.47	18.56	0.0035	
	34.293	1	34.29	85.16	<0.0001	
	12.956	1	12.96	32.17	0.0008	
	11.731	1	11.73	29.13	0.0010	
	64.070	1	64.07	159.11	<0.0001	
	5.440	1	5.44	13.51	0.0079	
	6.636	1	6.64	16.48	0.0048	
Residual	2.819	7	0.40			
Lack of fit	2.811	3	0.94	501.76	<0.0001	Significant
Pure error	0.007	4	0.00			
Cor total	260.214	16				

R^2=0.9892; Adjusted R^2=0.9752
Predicted R^2=0.8271; Adequate precision=33.735

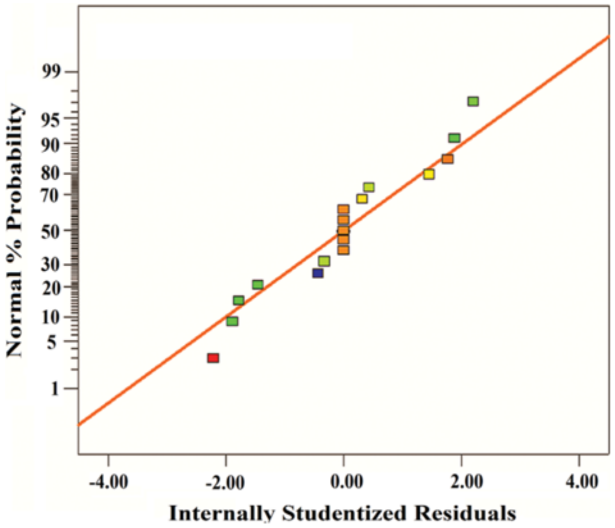

Fig. S1. Normal plot of residuals showing the relationship between normal probability (%) and internally studentized residuals for propionic acid conversion.

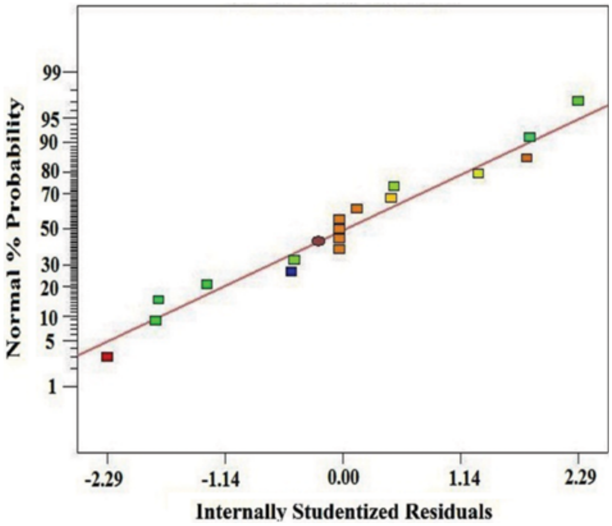

Fig. S2. Normal plot of residuals showing the relationship between normal probability (%) and internally studentized residuals for yield of ester.